A subset of oligodendrocytes generated from radial glia in the dorsal spinal cord

Matthew Fogarty, William D Richardson and Nicoletta Kessaris

The Wolfson Institute for Biomedical Research and Department of Biology, University College London (UCL), Gower Street, London WC1E 6BT, UK.

***Correspondence**:* Bill Richardson, tel +44 (0)20 7679 6729 w.richardson@ucl.ac.uk

Keywords: Dbx, Cre, spinal cord, radial glia, neurons, astrocytes, oligodendrocytes.

Running title: Dorsally-derived oligodendrocytes

Abstract (149 words)
Many oligodendrocytes in the spinal cord are derived from a region of the ventral ventricular zone (VZ) that also gives rise to motor neurons. Cell fate specification in this region depends on Sonic hedgehog (Shh) from the notochord and floor plate. There have been suggestions of an additional source(s) of oligodendrocytes in the dorsal spinal cord. We revisited this idea by Cre-lox fate-mapping in transgenic mice. We found that a subpopulation of oligodendrocytes is generated from the Dbx1-expressing domain of the VZ, spanning the dorsoventral midline. Dbx-derived oligodendrocytes comprise less than 5% of the total; they are formed late during embryogenesis by transformation of radial glia and settle mainly in the lateral white matter. Development of Dbx-derived oligodendrocytes in vitro can occur independently of Shh but requires FGF signalling. Dbx-expressing precursors also generate astrocytes and interneurons but do not contribute to the ependymal layer of the postnatal spinal cord.

Introduction
Most spinal cord oligodendrocytes are generated from proliferative, migratory progenitor cells that originate in the ventral neuroepithelium – specifically in the pMN domain, which also gives rise to motor neurons (MNs) (Warf et al., 1991; Pringle and Richardson, 1993; Yu et al., 1994; Timsit et al., 1995; Ono et al., 1995; Sun et al., 1998; Lu et al., 2002; Zhou and Anderson, 2002; Takebayashi et al., 2002; Agius et al., 2004; reviewed by Rowitch, 2004). Induction of oligodendrocyte progenitors (OLPs) is dependent on Sonic hedgehog (Shh) secreted from the notochord and floor plate at the ventral midline (Orentas et al., 1999; Poncet et al., 1996; Pringle et al., 1996). Shh induces expression of the basic helix-loop-helix transcription factor Olig2, which is required for generation of both MNs and OLPs (Lu et al., 2002; Zhou and Anderson, 2002; Takebayashi et al., 2002). Soon after OLPs are generated in the pMN domain, they migrate away in all directions, populating the spinal cord and maturing mainly in the white matter.

Evidence for a restricted ventral source of OLPs seems to conflict with other studies that favour more widespread generation of OLPs. For example, immunohistochemical studies have suggested that radial glial cells can transform into oligodendrocytes at the end of neuronogenesis; since radial glia are present in all regions of the embryonic spinal cord VZ this implies that oligodendrocyte generation might also be widespread (Choi et al., 1983; Choi and Kim, 1985; Hirano and Goldman, 1988). Furthermore, studies based on transgenic mice that express *lacZ* under transcriptional control of the myelin proteolipid protein (*PLP/DM20*) gene suggest that there might be additional dorsal sources of OLPs, at least in the cervical spinal cord and brainstem (Spassky et al., 1998). There are also contradictory

data from chick-quail chimeras that raise the possibility of dorsal as well as ventral sources of OLPs in birds (Cameron-Curry and Le-Douarin, 1995; Pringle et al., 1998; Richardson et al., 1997).

In the present study we used Cre-mediated recombination in transgenic mice to follow the neuronal and glial fates of neural precursors in a restricted part of the spinal cord neuroepithelium that expresses the transcription factor Dbx1. The initial expression of Dbx1 (and Dbx2) spans four adjoining domains of the neuroepithelium, two dorsal (dP5 and dP6) and two ventral (p0 and p1) (Pierani et al., 2001). We demonstrate that, in addition to the expected interneuron populations, both oligodendrocytes and astrocytes are generated from the Dbx1/2 domain. The appearance of Dbx-derived cells with a hybrid oligodendrocyte/ radial glial antigenic phenotype and a radial morphology suggests direct transformation of radial glia into oligodendrocytes, as suggested previously (Choi et al., 1983; Choi and Kim, 1985; Hirano and Goldman, 1988). The Dbx-derived oligodendrocytes comprise less than 5% of the total oligodendrocyte population in the cord and have a more restricted distribution, mainly settling in the lateral white matter radially opposite their point of origin. In addition to oligodendrocytes, the Dbx1/2 neuroepithelium generates at least two classes of astrocytes – fibrous astrocytes in the white matter and protoplasmic astrocytes in the gray.

Materials and Methods

Isolation and characterization of Dbx1 genomic clones

To identify clones containing the *Dbx1* locus we screened a mouse genomic phage artificial chromosome (PAC) library (RCPI 21 from the UK HGMP resource centre) with a probe spanning the 3' UTR sequence of *Dbx1* (derived from IMAGE clone 426959 by *BamH*I and *Not*I digest). Six PAC clones were isolated and characterized by restriction enzyme mapping and pulsed field gel electrophoresis (PFGE). The extremities of the PAC inserts were further confirmed by inverse PCR cloning and DNA sequencing. PAC 631-M19, which contained a genomic fragment 235 kb in length (Fig. 1A), was used to generate transgenic mice.

PAC modification and generation of Dbx1-iCre transgenic mice

The targeting vector used to modify PAC 631-M19 is shown in Fig. 1C. The 5' and 3' homology regions were amplified by PCR from the PAC clone using Expand High Fidelity Taq Polymerase (Roche). The codon-improved Cre recombinase (iCre) (Shimshek et al., 2002) with a nuclear localization signal attached was fused to the initiation codon of Dbx1 using a PCR-based approach. A chloramphenicol resistance cassette flanked by *loxP* sites was inserted between iCre and the 3' homology to allow for selection of the correctly recombined clones. PAC modification was carried out in a bacterial system as previously

described (Lee et al., 2001), thereby removing the entire coding region of Dbx1 and replacing it with iCre.

The modified PAC DNA was linearized by *Asc*I digestion. PFGE was used to purify the PAC insert away from small vector fragments. This linear PAC DNA was concentrated into a 4% low melting point agarose gel. Following β-agarase (New England Biolabs) digestion and dialysis with microinjection buffer, the DNA was injected into pronuclei of fertilized mouse eggs. Transgenic mouse pups were screened for the presence of the *Dbx1-iCre* transgene by PCR and Southern blotting (primer sequences available on request).

In situ hybridization and immunohistochemistry

Embryos were fixed in 4% (w/v) paraformaldehyde (PFA) in phosphate-buffered saline (PBS). Generally, material was fixed overnight for in situ hybridization while fixation times for immunohistochemistry were varied according to the age of the embryo and the epitope in question. Fixed embryos were cryoprotected overnight in 20% (w/v) sucrose in PBS. Postnatal animals were perfused with 4% (w/v) PFA through the right ventricle of the heart under terminal anaesthesia. All tissues were embedded in Tissue-Tek OCT compound (R.A. Lamb Ltd.) and frozen on dry ice. Sections (5 to 15 μm) were cut on a cryostat and collected on Superfrost Plus glass slides (BDH).

All solutions used for in situ hybridization were pre-treated with diethyl pyrocarbonate (0.1% v/v). The following plasmids were used to generate digoxigenin-labelled probes: mouse Dbx1, a 2 kb fragment spanning the 3' end of the coding sequence and the entire 3' UTR, from IMAGE clone 426959 (UK HGMP resource centre); mouse Dbx2, a 500 bp PCR product that includes parts of the final exon and the 3'UTR; mouse Olig2, a 1.7 kb 3' *BamH*I - *Nco*I fragment downstream of the open reading frame; mouse Nkx6.1, a 2.2 kb full length cDNA (gift from T. Jessell); and Mash1, a 700 bp fragment that includes most of the coding sequence and part of the 3' UTR, from IMAGE clone 481779 (UK HGMP resource centre). Details of the in situ hybridization techniques have been described previously (Pringle et al., 1996; Fruttiger et al., 1999) (http://www.ucl.ac.uk/~ucbzwdr/MandM.htm)

For immunohistochemistry the antibodies used were: rabbit anti-GFP at 1:8000 dilution (AbCam); rabbit anti-Olig2 (a gift from D.Rowitch); mouse monoclonal anti-RC2 IgM at 1:5 dilution (Developmental Studies Hybridoma Bank, DSHB); rat anti-PDGFRα at 1:500 (BD Biosciences); mouse monoclonal anti-GFAP at 1:400 (Sigma); guinea-pig anti-Sox10 at 1:2000 (a gift from M. Wegner); monoclonal anti-NeuN at 1:400 (Chemicon); monoclonal anti-Pax7 at 1:10 (DSHB); monoclonal pan-Islet 4D5 at 1:20 (DSHB); guinea-pig anti-Evx1 at

1:8000 (a gift from T. Jessell); monoclonal CC1 at 1:400 (Merck Biosciences); guinea pig anti-Lbx1 at 1:8000 (gift from T. Jessell); monoclonal anti-Lim2 at 1:5 (DSHB); monoclonal anti-Lim3 at 1:20 (DSHB) and monoclonal anti-S100β at 1:400 (Sigma). Primary antibodies were applied overnight at 4°C. Secondary antibodies were rhodamine- , AMCA- or fluorescein- conjugated anti-rabbit, -goat, -rat, -guinea pig or -mouse IgM or anti-mouse IgG at 1:200 (Pierce) and were applied for 60 minutes at room temperature. To allow Olig2 and GFP double labelling, a goat anti-rabbit IgG Fab fragment (Jackson) was used to effectively convert rabbit Olig2 into a goat antibody, prior to detection with an anti-goat IgG secondary antibody. All antibodies were diluted in PBS containing 10% serum and 0.1% (v/v) Triton X-100. Following antibody treatment, sections were stained with Hoescht (Sigma) and post-fixed for 5 minutes in 4% PFA. Sections were mounted under coverslips in Citifluor anti-fade reagent (City University, UK).

Spinal cord cultures

Spinal cord cultures were done as previously described (Kessaris et al, 2004). Briefly, spinal cords from E12.5 mouse embryos were dissected away from surrounding tissue in Hepes-buffered minimal essential medium (MEM-H) (Invitrogen) and dissociated by incubation in 0.0125% (w/v) trypsin in Earle's balanced salt solution (EBSS, Invitrogen) for 30 minutes at 37^{o}C in 5% CO_2. The cells were mechanically dissociated in the presence of DNaseI and seeded onto 13 mm poly-D-lysine-coated coverslips in a 50 μl droplet of Dulbecco's modified Eagle's medium (DMEM, Invitrogen) containing 0.5% FCS at a density of 2.5x10^5 cells/coverslip. The cells were allowed to attach for 30 minutes. 350 μl of defined medium (Bottenstein and Sato, 1979) was added and incubation continued at 37^{o}C in 5% CO_2. Cyclopamine was used at a final concentration of 1 μM and the FGFR inhibitor PD173074 at 100 nM.

Results

Generation of Dbx1-iCre transgenic mice

To generate mice expressing Cre recombinase under *Dbx1* transcriptional control we used PAC transgenics. A 230 kb PAC (RP21-631-M19) containing 147 kb upstream and 85 kb downstream of the Dbx1 gene was modified to replace the coding region of Dbx1 with that of iCre (Lee et al., 2001) (Fig. 1A-C and Methods). The modified PAC insert was purified and microinjected into fertilized mouse eggs. Three independent transgenic lines were generated, all of which showed similar expression of the transgene in a pattern resembling that of the endogenous Dbx1 (Fig. 1D). From E9.5 to E15.5 expression was restricted to a

small region of the neuroepithelium. From E16.5 onwards all transcript expression was abolished (data not shown). We selected one of these lines for further study.

To establish the dorsal and ventral limits of Cre expression in the neuroepithelium, we crossed the *Dbx1-Cre* mice to the *Rosa26-GFP* reporter line (Mao et al., 2001) and analyzed the offspring at embryonic day 10.5 (E10.5) by in situ hybridization. GFP expression was activated in a broad neuroepithelial domain, wider than the domain of *Dbx1* expression at the same age but corresponding more closely to *Dbx2* (Fig. 2A-C). This is consistent with previous reports that *Dbx1* is initially expressed (prior to E10.5) in an identical pattern to *Dbx2* and only narrows down later (Pierani et al., 2001). The region of GFP activation therefore probably corresponds to the early *Dbx1/ Dbx2* co-expression domain. The ventral limit of GFP expression abuts the dorsal limit of *Nkx6.1*, many cell diameters away from the *Olig2*-expressing domain in pMN (Fig. 2D-F). This is consistent with previous data showing mutually exclusive expression of Nkx6.1 and Dbx2 in the spinal cord (Briscoe et al., 2000). The dorsal limit of GFP activation overlaps with Mash1 and Pax7 which are expressed within dP5 or dP6, respectively, at their ventral limit (Fig. 2G-I) (Caspary and Anderson, 2003; Helms and Johnson, 2003). Collectively, the data demonstrate that expression of iCre is restricted to *Dbx1/Dbx2*-positive neuroepithelial precursors and activation of the GFP reporter gene is therefore restricted to four domains of the neuroepithelium: dP5, dP6, P0 and P1 (Fig. 1E).

We examined the distribution of GFP in *Dbx1-iCre x Rosa26-GFP* embryos around the time of neurogenesis in the spinal cord (E12.5). At E12.5, GFP-labelled cells were found exclusively in the ventral and lateral spinal cord (Fig. 3A). GFP-labelled axons were observed in the developing ventral white matter, including commissural axon tracts (Fig. 3A). Subsets of GFP-labelled neurons in the lateral cord co-expressed Lbx1, which marks early postmitotic neurons derived from dP4, dP5 and dP6 (Muller et al., 2002) (Fig. 3D). Other GFP-labelled neurons in the ventral spinal cord expressed Evx1, which marks neurons derived from the p0 domain (Moran-Rivard et al., 2001) (Fig. 3E) and En1, which marks V1 interneurons in the lateral cord (not shown) (Saueressig et al., 1999). The majority of the GFP-labelled cells observed in the spinal cord at this stage co-expressed the homeodomain transcription factor Lim2 (Fig. 3F), which is expressed in a variety of postmitotic neurons (Tsuchida et al., 1994).

In contrast, there was no co-expression of GFP in Isl1/ Isl2-positive neurons derived from pMN or dP3 (Fig. 3B) (Tsuchida et al., 1994) or in Lim3-positive interneurons derived from p2 or motor neurons from pMN (Fig. 3C) (Tsuchida et al., 1994). In conclusion, and as

predicted from previous studies, the *Dbx*-expressing neuroepithelium gives rise to at least four recognizable neuronal subtypes that have different distributions, different antigenic phenotypes and presumably distinct functions within the spinal cord.

Radial glia are generated from the Dbx neuroepithelium

Radial glia were one of the first cell types to express GFP in *Dbx1-Cre x Rosa26-GFP* offspring (Fig. 4A-F). They had a typical radial glial morphology with a single thin process extending from the ventricular zone all the way to the pial surface (reviewed by Bentivoglio and Mazzarello, 1999). Immuno-labelling with monoclonal antibody RC2 showed co-localization along the entire length of the process (Fig. 4A-F). Co-expression of RC2 and GFP persisted throughout embryogenesis. The morphology of these cells changed with time, however. From E15.5, an increasing number of (RC2, GFP) double-labelled cells appeared to translocate their cell bodies close to the pial surface (shown in Fig. 4G-L at E16.5) and to change their antigenic profile (see below). We thought it possible that these might correspond to radial glial cells in the process of transforming into astrocytes and/or oligodendrocytes at the end of neuronogenesis (Schmechel and Rakic, 1979; Choi et al., 1983; Choi and Kim, 1985; Hirano and Goldman, 1988; Voigt, 1989).

Oligodendrocytes are generated from the Dbx neuroepithelium

We immunolabeled spinal cord sections from *Dbx1-Cre x Rosa26-GFP* offspring for GFP together with either Olig2 or Sox10, markers of the oligodendrocyte lineage. Starting around E15.5, cells with a GFP-labelled radial process reminiscent of a radial glial cell and either an Olig2- or a Sox10-positive nucleus were found near the pial surface (Fig. 5A-B). At this stage Olig2 expression was observed in approximately 25% of the radially-orientated GFP-positive cells. Triple immunolabelling with RC2, anti-GFP and either anti-Sox10 or anti-Olig2 showed co-localization of all three markers in a small subset of cells suggesting that these represent oligodendrocyte lineage cells arising directly from radial glia (Fig. 5E-P). These triple-labelled cells were infrequent (18% of the Olig2+/GFP+ radial cells), consistent with them being in a transitional state. The radially-orientated appearance of GFP-labelled oligodendrocyte lineage cells was maintained until late embryogenic stages (Fig. 5C-D).

To further confirm the oligodendroglial identity of these cells and determine their distribution at later developmental stages we looked in postnatal spinal cords 10 days after birth (P10). GFP-expressing oligodendrocytes and OLPs, identified by immunolabelling with anti-Sox10, anti-Pdgfra or monoclonal antibody CC1 were concentrated in white matter, mainly in the lateral funiculus although rare cells also were present in the dorsal and ventral funiculi (Fig. 6 and not shown). At this stage they had a more rounded cell body with multiple

processes, typical of maturing oligodendrocytes. They comprised around 3% of the total Sox10-expressing oligodendroglial cells in the spinal cord at P10.

The *Rosa26* promoter remains active in adult *Rosa26-GFP* mice but its activity is reduced and GFP is difficult to detect by immunohistochemistry. Therefore, to determine the contribution of *Dbx*-derived oligodendrocytes to the adult spinal cord we switched to using the Rosa26-lacZ reporter strain (Soriano 1999). β-gal positive cells were observed throughout the spinal cord and especially in the white matter, in a distribution similar to that at earlier stages, indicating that *Dbx*-derived oligodendrocytes make a limited contribution to the oligodendrocyte population of the adult spinal cord (data not shown).

Oligodendrocyte generation from Dbx-expressing precursors is independent of Shh signalling

The *Dbx*-expressing neuroepithelium is exposed to low levels of Shh in vivo and neuronal specification within the *Dbx* domain depends on signals other than Shh (Pierani et al., 1999). The emergence of oligodendrocytes from this region was therefore surprising given the known requirement for Shh in specifying OLPs in the ventral pMN domain. FGF has recently been shown to be capable of promoting oligodendrocyte specification in cultures of neural precursors from embryonic cerebral cortex or spinal cord (Chandran et al, 2003; Kessaris et al, 2004). To determine the signalling requirements for generation of *Dbx*-derived oligodendrocytes in vitro we dissociated embryonic spinal cords from *Dbx1-iCre x Rosa26-GFP* mice at E12.5 - approximately three days before the first appearance of *Dbx*-derived oligodendrocyte lineage cells in vivo - and cultured the cells in the presence of the hedghog inhibitor cyclopamine (Cooper et al 1998; Incardona et al, 1998) or the Fgfr inhibitor PD173074 (Skaper et al, 2000). In the absence of any inhibitors, GFP-labelled oligodendrocytes - identified by co-labelling with anti-Sox10 - developed in vitro within 5 days (Fig. 7A, 7E). Their development was not inhibited by cyclopamine (Fig. 7B, 7E) but was completely abolished by PD173074 (Fig. 7C-E), indicating a strict requirement for FGF signalling.

Two types of astrocytes from the Dbx neuroepithelium

In addition to oligodendrocytes and interneurons, two types of astrocytes were generated from the *Dbx*-expressing neuroepithelium (Fig. 8) – GFAP-positive “fibrous” astrocytes in the lateral funiculus (Fig. 8A-B) and “protoplasmic” astrocytes in the gray matter (Fig. 8A-F). The position and arrangement of *Dbx*-derived fibrous astrocytes was reminiscent of the distal ends of the radial glial processes suggesting that they, like oligodendrocytes, might be generated directly from radial glia by trans-differentiation (Voigt, 1989). Protoplasmic astrocytes had a very complex morphology with a small cell body and an extensive network

of fine branched processes labelled with GFP Fig. 8C-F). Some protoplasmic astrocytes co-labelled weakly with anti-GFAP (Fig. 8D) and all expressed S100β (Fig. 8C). They were interspersed among dorsal neurons (not shown) and motor neurons (Fig. 8E). They also formed bilateral, longitudinal columns of cells positioned adjacent to the central canal (arrows, Fig. 8F). They did not express NeuN (Fig. 8E, F) or Sox10 (not shown). It was noteworthy that there was no contribution from *Dbx*-derived cells to the ependymal layer of the postnatal spinal cord (Fig. 8D).

Discussion

Using transgenic mice that express Cre recombinase under *Dbx1* control we fate-mapped a discrete region of the spinal cord neuroepithelium near the dorso-ventral midline and found that it generates a subpopulation of oligodendrocytes. *Dbx*-derived OLPs appeared about three days later than the majority of OLPs - which are generated from the pMN domain starting on E12.5 - and had a more limited distribution. Their initial morphology and antigenic profile resembled radial glia, suggesting that they are formed by trans-differentiation of radial glia. Unlike their ventrally-derived counterparts, specification of *Dbx*-derived OLPs in vitro was independent of Shh but required FGF signalling. However, like pMN-derived OLPs they must require *Olig* gene function because oligodendrocyte lineage cells are completely absent from the spinal cords of *Olig2* or *Olig2/Olig1* compound knockout mice (Lu et al., 2002; Takebayashi et al., 2002; Zhou and Anderson, 2002). In keeping with this, we found that *Dbx*-derived oligodendrocytes, like those from pMN, also expressed Olig2.

A source(s) of oligodendrocytes outside pMN

Our experiments show unequivocally that some oligodendrocytes are generated from the Dbx neuroepithelial domain. We estimate that the *Dbx*-derived population comprises around 3% of all Sox10-positive oligodendrocyte lineage cells. This might be an underestimate, for not all of the neuroepithelial cells in the *Dbx* domain were GFP-labelled in all sections, presumably because of the transient nature of Dbx1-iCre expression. However, a majority of *Dbx*-expressing neuroepithelial cells was always labelled so we think it unlikely that their real contribution to oligodendrocyte production is more than 5%. Most of the remainder presumably come from pMN, although further sub-populations of oligodendrocytes might turn out to be derived from outside either pMN or the *Dbx* domain (for summary see Fig. 9). It would be interesting to determine whether the *Dbx*-derived oligodendrocytes are functionally different from the rest. They are found predominantly in the lateral white matter suggesting that their progenitors might migrate less widely than the majority.

There have been previous suggestions of a dorsal source(s) of oligodendrocytes in the rodent cervical spinal cord and hindbrain, based on early expression of the myelin proteolipid protein (PLP/DM20) or expression of a *PLP/DM-20-lacZ* transgene (Spassky et al., 1998; Spassky et al., 2000). No estimate could be made of the relative contributions of dorsal versus ventral sources in those studies. A previous fate-mapping study from our laboratory using chick-quail chimeras suggested that oligodendrocytes develop only from ventral grafts (Pringle et al., 1998), although Cameron-Curry and Le Douarin (1995) concluded from similar experiments that oligodendrocytes are generated from all parts of the neuroepithelium. It might be that Pringle et al (1998) overlooked a small number of dorsally-derived oligodendrocytes. Alternatively, the dorsal source of oligodendrocytes might be present in rodents but not birds.

The dorsally-derived oligodendrocyte lineage cells expressed the same markers as their ventrally-derived counterparts - at least those we tested (Olig2, Sox10, Pdgfra and CC1). Thus we found no evidence so far that the dorsally-derived subpopulation is antigenically distinct.

Shh-independent oligodendrogenesis in the dorsal spinal cord

Shh released from the floor plate and notochord is essential for development of OLPs in the ventral spinal cord. Chandran et al. (2003) recently showed that neural stem cells derived from dorsal spinal cord can be induced by FGF2 to generate OLPs in vitro. The same was shown for embryonic cortical precursors by Kessaris et al. (2004). In this study we made use of *Dbx1-Cre* x *Rosa26-GFP* mice to identify neural precursors derived specifically from the *Dbx* domain in embryonic spinal cord cultures. Our experiments showed that OLPs can develop from *Dbx*-derived precursors independently of Shh (i.e. not inhibited by cyclopamine), consistent with a previous report of Shh-independent specification of interneurons in this region (Pierani et al., 1999). We also showed that OLP development from Dbx-positive spinal cord precursors requires FGF signalling in vitro. To discover whether FGF signalling is actually implicated in vivo would require specific inhibition of FGF signalling in the dorsal spinal cord – difficult to contemplate at present because we do not know which of the large number of FGF family members is involved or indeed which FGF receptor.

The relationship between radial glia and oligodendrocytes

Some of the first cells to be labelled with GFP in our reporter mice were radial glia. The nuclei of these cells are initially located in or close to the VZ and their radial processes extend to the pial surface. By analogy with radial glia in the brain, it seems likely that they

correspond to the neuroepithelial precursors themselves (Malatesta et al., 2003; Anthony et al., 2004). From E15.5, when the radial glial cell bodies moved towards the pial surface, we observed co-expression of RC2 and the oligodendrocyte lineage markers Olig2 or Sox10 in some radially-oriented cells, suggesting that the radial glia transform directly into oligodendrocytes. This supports previous evidence that spinal cord radial glia can give rise to oligodendrocytes as well as astrocytes after neuron generation has ceased (Choi et al., 1983; Choi and Kim, 1985; Hirano and Goldman, 1988).

It is not clear whether the mode of OLP generation from *Dbx* expressing precursors is fundamentally different from their mode of generation in the ventral cord. pMN-derived OLPs are presumably derived from radial glia too, since the latter are now thought to correspond to stem cells that generate all the neurons and glia of the CNS. However, the pMN-derived OLPs arise close to the ventricular surface whereas we first detected *Dbx*-derived OLPs towards the pial surface. This presumably relates to the position of the radial glial cell bodies at the time they start to express oligodendrocyte lineage markers such as Pdgfra, Sox10 or Olig2. Another difference seems to lie in how widely the OLPs disseminate after they are formed; those formed early from pMN proliferate rapidly at first and migrate away from pMN in all directions whereas the later-forming Dbx-derived OLPs proliferate less strongly, if at all, and migrate less widely. It remains to be determined whether these different behaviours reflect different inducing signals (Shh versus FGF, say), different environments in the cord at early versus late embryonic stages, or some intrinsic difference between the ventral and dorsal subsets.

Two types of astrocytes are generated from the Dbx domain

In addition to interneurons and oligodendrocytes, at least two morphological subtypes of astrocytes were generated from the *Dbx* domain. Protoplasmic astrocytes had a typical spherical outline with an extensive and intricate network of sheet-like branching processes and were distributed widely within the gray matter of the spinal cord. They were frequently associated with the cell bodies of neurons in both the dorsal and ventral cord, including motor neurons. Fibrous astrocytes on the other hand had a restricted distribution within the lateral white matter - in those regions previously occupied by the distal ends of the radial glia processes. The latter observation is consistent with the idea that some radial glia transform directly into fibrous astrocytes at the end of neuronogenesis (Schmechel and Rakic, 1979; Voigt, 1989; see Goldman, 2001 for review).

Our *Dbx1-iCre* mice label the progeny of four neuroepithelial domains – p1, p0, dP6 and dP5 – so we cannot tell whether each one of these domains generates all of the glial cell types

described here or whether different subsets of glia are generated from each individual domain, as has been shown for neurons. Resolution of this question would require targeting of the Cre transgene to individual neuroepithelial domains within the broader Dbx domain - not possible with currently available Cre deleter strains.

Dbx-neuroepithelial cells do not generate ependymal cells

We observed that *Dbx1/ Dbx2* precursors do not contribute to the ependymal layer that surrounds the reduced lumen of the postnatal and adult spinal cord, adding to previous evidence that ependymal cells are derived entirely from ventral (Nkx6.1-expressing) neuroepithelium (Richardson et al., 1997; Fu et al., 2003). Nevertheless, a subset of the *Dbx*-derived protoplasmic astrocytes settles close to the postnatal ependymal layer where they form narrow bilateral columns of cells along the length of the spinal cord. It is interesting to speculate that these might correspond to a subset of "subependymal astrocytes" analogous to those that have been described as neural stem cells in the postnatal telencephalon (Doetsch et al., 1999).

Acknowledgements

We thank Matthew Grist for technical assistance, Ulla Dennehy and Palma Iannarelli for transgenic mouse production and our colleagues for useful discussions. We also thank Tom Jessell, David Rowitch, Michael Wegner, Rolf Sprengel and Neal Copeland for antibodies and plasmids, Jaime Carvajal for advice about PAC recombination and Nigel Pringle for help with immunohistochemistry. We thank Stephen Skaper for PD173074 and William Gaffield for cyclopamine. Work in the authors' laboratory is supported by the Wellcome Trust Functional Genomics Initiative, the UK Medical Research Council and a Wellcome Trust Studentship to Matthew Fogarty.

Note added in proof

While this article was being reviewed, two other articles were published that demonstrate production of a subset of oligodendrocyte precursors in the dorsal VZ (dP3, dP4 and dP5) [**Cai, J., Qi, Y., Hu, X., Tan, M., Liu, Z., Zhang, J., Li, Q., Sander, M., and Qiu, M.** (2005). Generation of oligodendrocyte precursor cells from mouse dorsal spinal cord independent of *Nkx6l*-regulation and *Shh* signalling. *Neuron* **45**, 41-53; **Vallstedt, A., Klos, J.M., and Ericson, J.** (2005). Multiple dorsoventral origins of oligodendrocyte generation in the spinal cord and hindbrain. *Neuron* **45**, 55-67; reviewed by **Miller, R.H.** (2005). Dorsally derived oligodendrocytes come of age. *Neuron* **45**, 1-3.]

References

Agius, E., Soukkarieh, C., Danesin, C., Kan, P., Takebayashi, H., Soula, C., and Cochard, P. (2004). Converse control of oligodendrocyte and astrocyte lineage development by Sonic hedgehog in the chick spinal cord. *Dev. Biol.* **270,** 308-321.

Anthony, T. E., Klein, C., Fishell, G., and Heintz, N. (2004). Radial glia serve as neuronal progenitors in all regions of the central nervous system. *Neuron* **41,** 881-890.

Bentivoglio, M. and Mazzarello, P. (1999). The history of radial glia. *Brain Res. Bull.* **49,** 305-315.

Bhat, R. V., Axt, K. J., Fosnaugh, J. S., Smith, K. J., Johnson, K. A., Hill, D. E., Kinzler, K. W., and Baraban, J. M. (1996). Expression of the APC tumor suppressor protein in oligodendroglia. *Glia* **17,** 169-174.

Briscoe, J., Pierani, A., Jessell, T. M., and Ericson, J. (2000). A homeodomain protein code specifies progenitor cell identity and neuronal fate in the ventral neural tube. *Cell* **101,** 435-445.

Cameron-Curry, P. and Le Douarin, N.M. (1995). Oligodendrocyte precursors originate from both the dorsal and the ventral parts of the spinal cord. *Neuron* **15**, 1299-1310.

Caspary, T. and Anderson, K. V. (2003). Patterning cell types in the dorsal spinal cord: what the mouse mutants say. *Nat. Rev. Neurosci.* **4,** 289-297.

Chandran, S., Kato, H., Gerreli, D., Compston, A., Svendsen, C. N., and Allen, N. D. (2003). FGF-dependent generation of oligodendrocytes by a hedgehog-independent pathway. *Development* **130,** 6599-6609.

Choi, B. H., Kim, R. C., and Lapham, L. W. (1983). Do radial glia give rise to both astroglial and oligodendroglial cells? *Dev. Brain Res.* **8,** 119-130.

Choi, B. H. and Kim, R. C. (1985). Expression of glial fibrillary acidic protein by immature oligodendroglia and its implications. *J. Neuroimmunol.* **8,** 215-235.

Cooper, M.K., Porter, J.A., Young, K.E. and Beachy, P.A. (1998). Teratogen-mediated inhibition of target tissue response to Shh signaling. *Science* **280**, 1603-1607.

Doetsch, F., Caille, I., Lim, D. A., Garcia-Verdugo, J. M., and Alvarez-Buylla, A. (1999). Subventricular zone astrocytes are neural stem cells in the adult mammalian brain. *Cell* **97,** 703-716.

Fruttiger, M., Karlsson, L., Hall, A. C., Abramsson, A., Calver, A. R., Bostrom, H., Willetts, K., Bertold, C. H., Heath, J. K., Betsholtz, C., and Richardson, W.D. (1999). Defective oligodendrocyte development and severe hypomyelination in PDGF-A knockout mice. *Development* **126,** 457-467.

Fu, H., Qi, Y., Tan, M., Cai, J., Hu, X., Liu, Z., Jensen, J., and Qiu, M. (2003). Molecular mapping of the origin of postnatal spinal cord ependymal cells: evidence that adult ependymal cells are derived from Nkx6.1+ ventral neural progenitor cells. *J. Comp Neurol.* **456,** 237-244.

Goldman, J. E. (2001). Developmental origins of astrocytes. In *Glial cell development*. (ed. Jessen,K.R. and Richardson,W.D.), pp. 55-74. Oxford, New York: Oxford Univerity Press.

Helms, A. W. and Johnson, J. E. (2003). Specification of dorsal spinal cord interneurons. *Curr. Opin. Neurobiol.* **13,** 42-49.

Hirano, M. and Goldman, J. E. (1988). Gliogenesis in the rat spinal cord: Evidence for origin of astrocytes and oligodendrocytes from radial precursors. *J. Neurosci. Res.* **21,** 155-167.

Incardona, J.P., Gaffield, W., Kapur, R.P. and Roelink H. (1998). The teratogenic Veratrum alkaloid cyclopamine inhibits sonic hedgehog signal transduction. *Development* **125**, 3553-3562.

Kessaris, N., Jamen, F., Rubin, L. L., and Richardson, W. D. (2004). Cooperation between sonic hedgehog and fibroblast growth factor/MAPK signalling pathways in neocortical precursors. *Development* **131,** 1289-1298.

Lee, E. C., Yu, D., Martinez, D. V, Tessarollo, L., Swing, D. A., Court, D. L, Jenkins, N. A., and Copeland, N. G. (2001). A highly efficient Escherichia coli-based chromosome engineering system adapted for recombinogenic targeting and subcloning of BAC DNA. *Genomics* **73,** 56-65.

Lu, Q. R., Sun, T., Zhu, Z., Ma, N., Garcia, M., Stiles, C. D., and Rowitch, D. H. (2002). Common developmental requirement for Olig function indicates a motor neuron/ oligodendrocyte connection. *Cell* **109,** 75-86.

Malatesta, P., Hack, M. A., Hartfuss, E., Kettenmann, H., Klinkert, W., Kirchhoff, F., and Gotz, M. (2003). Neuronal or glial progeny: regional differences in radial glia fate. *Neuron* **37,** 751-764.

Mao, X., Fujiwara, Y., Chapdelaine, A., Yang, H., and Orkin, S. H. (2001). Activation of EGFP expression by Cre-mediated excision in a new ROSA26 reporter mouse strain. *Blood* **97,** 324-326.

Moran-Rivard, L., Kagawa, T., Saueressig, H., Gross, M. K., Burrill, J., and Goulding, M. (2001). Evx1 is a postmitotic determinant of V0 interneuron identity in the spinal cord. *Neuron* **29,** 385-399.

Muller, T., Brohmann, H., Pierani, A., Heppenstall, P. A., Lewin, G. R., Jessell, T. M., and Birchmeier, C. (2002). The homeodomain factor Lbx1 distinguishes two major programs of neuronal differentiation in the dorsal spinal cord. *Neuron* **34,** 551-562.

Ono, K., Bansal, R., Payne, J., Rutishauser, U., and Miller, R. H. (1995). Early development and dispersal of oligodendrocyte precursors in the embryonic chick spinal cord. *Development* **121,** 1743-1754.

Orentas, D. M., Hayes, J. E., Dyer, K. L., and Miller, R. H. (1999). Sonic hedgehog signaling is required during the appearance of spinal cord oligodendrocyte precursors. *Development* **126,** 2419-29.

Peters, A., Palay, S. L., and Webster, H. d. F. (1991). *The fine structure of the nervous system*. Oxford: Oxford University Press.

Pierani, A., Brenner-Morton, S., Chiang, C., Jessel, TM. (1999) A sonic hedgehog-independent, retinoid-activated pathway of neurogenesis in the ventral spinal cord. *Cell*. **7**, 903-15.

Pierani, A., Moran-Rivard, L., Sunshine, M. J., Littman, D. R., Goulding, M., and Jessell, T. M. (2001). Control of interneuron fate in the developing spinal cord by the progenitor homeodomain protein Dbx1. *Neuron* **29,** 367-384.

Poncet, C., Soula, C., Trousse, F., Kan, P., Hirsinger, E., Pourquié, O., Duprat, A.-M., and Cochard, P. (1996). Induction of oligodendrocyte precursors in the trunk neural tube by ventralizing signals: effects of notochord and floor plate grafts, and of sonic hedgehog. *Mech. Dev.* **60,** 13-32.

Pringle, N. P. and Richardson, W. D. (1993). A singularity of PDGF alpha-receptor expression in the dorsoventral axis of the neural tube may define the origin of the oligodendrocyte lineage. *Development* **117,** 525-533.

Pringle, N. P., Yu, W.-P., Guthrie, S., Roelink, H., Lumsden, A., Peterson, A. C., and Richardson, W. D. (1996). Determination of neuroepithelial cell fate: induction of the oligodendrocyte lineage by ventral midline cells and sonic hedgehog. *Dev. Biol.* **177,** 30-42.

Pringle, N. P., Guthrie, S., Lumsden, A., and Richardson, W. D. (1998). Dorsal spinal cord neuroepithelium generates astrocytes but not oligodendrocytes. *Neuron* **20,** 883-893.

Pringle, N. P., Yu, W.-P., Howell, M., Colvin, J. S., Ornitz, D. M., and Richardson, W. D. (2003). Fgfr3 expression by astrocytes and their precursors: evidence that astrocytes and oligodendrocytes originate in distinct neuroepithelial domains. *Development* **130,** 93-102.

Richardson, W. D., Pringle, N. P., Yu, W.-P., and Hall, A. C. (1997). Origins of spinal cord oligodendrocytes: possible developmental and evolutionary relationships with motor neurons. *Dev. Neurosci.* **19,** 58-68.

Richardson, W. D., Smith, H. K., Sun, T., Pringle, N. P., Hall, A., and Woodruff, R. (2000). Oligodendrocyte lineage and the motor neuron connection. *Glia* **29,** 136-142.

Rowitch, D. H. (2004). Glial specification in the vertebrate neural tube. *Nat. Rev. Neurosci.* **5**, 409-419.

Saueressig, H., Burrill, J., and Goulding, M. (1999). Engrailed-1 and netrin-1 regulate axon pathfinding by association interneurons that project to motor neurons. *Development* **126,** 4201-4212.

Schmechel, D. E. and Rakic, P. (1979). A Golgi study of radial glial cells in developing monkey telencephalon: morphogenesis and transformation into astrocytes. *Anat. Embryol. (Berl)* **156,** 115-152.

Shimshek, D. R., Kim, J., Hubner, M. R., Spergel, D. J., Buchholz, F., Casanova, E., Stewart, A. F., Seeburg, P. H., and Sprengel, R. (2002). Codon-improved Cre recombinase (iCre) expression in the mouse. *Genesis.* **32,** 19-26.

Skaper, S.D., Kee, W.J., Facci, L., Macdonald, G., Doherty, P. and Walsh, F.S. (2000). The FGFR1 inhibitor PD 173074 selectively and potently antagonizes FGF-2 neurotrophic and neurotropic effects. *J Neurochem*. **754**, 1520-1527.

Soriano, P. (1999). Generalised lacZ expression with the ROSA26 Cre reporter strain. *Nat. Genet.* **1**, 70-1.

Spassky, N., Goujet-Zalc, C., Parmantier, E., Olivier, C., Martinez, S., Ivanova, A., Ikenaka, K., Macklin, W., Cerruti, I., Zalc, B., and Thomas, J.-L. (1998). Multiple restricted origin of oligodendrocytes. *J. Neurosci.* **18,** 8331-8343.

Spassky, N., Olivier, C., Perez-Villegas, E., Goujet-Zalc, C., Martinez, S., Thomas, J., and Zalc, B. (2000). Single or multiple oligodendroglial lineages: a controversy. *Glia* **29,** 143-148.

Sun, T., Pringle, N. P., Hardy, A. P., Richardson, W. D., and Smith, H. K. (1998). Pax6 inluences the time and site of origin of glial precursors in the ventral neural tube. *Mol. Cell. Neurosci.* **12,** 228-239.

Takebayashi, H., Nabeshima, Y., Yoshida, S., Chisaka, O., Ikenaka, K., and Nabeshima, Y. (2002). The basic helix-loop-helix factor Olig2 is essential for the development of motoneuron and oligodendrocyte lineages. *Curr. Biol.* **12,** 1157-1163.

Timsit, S., Martinez, S., Allinquant, B., Peyron, F., Puelles, L., and Zalc, B. (1995). Oligodendrocytes originate in a restricted zone of the embryonic ventral neural tube defined by DM-20 mRNA expression. *J. Neurosci.* **15,** 1012-1024.

Tsuchida, T., Ensini, M., Morton, S.B., Baldassare, M., Edlund, T., Jessell, T.M., and Pfaff, S.L. (1994). Topographic organization of embryonic motor neurons defined by expression of LIM homeobox genes. *Cell* **79,** 957-970.

Voigt, T. (1989). Development of glial cells in the cerebral wall of ferrets: direct tracing of their transformation from radial glia into astrocytes. *J. Comp Neurol.* **289,** 74-88.

Warf, B. C., Fok-Seang, J., and Miller, R. H. (1991). Evidence for the ventral origin of oligodendrocyte precursors in the rat spinal cord. *J. Neurosci.* **11,** 2477-2488.

Yu, W.-P., Collarini, E. J., Pringle, N. P., and Richardson, W. D. (1994). Embryonic expression of myelin genes: evidence for a focal source of oligodendrocyte precursors in the ventricular zone of the neural tube. *Neuron* **12,** 1353-1362.

Zhou, Q. and Anderson, D. J. (2002). The bHLH transcription factors OLIG2 and OLIG1 couple neuronal and glial subtype specification. *Cell* **109,** 61-73.

Figure Legends

Figure 1 Generation of *Dbx1-iCre* PAC transgenic mice and expression of the transgene. (A) Map of PAC 631-M19 indicating the extent of upstream and downstream genomic regions in the PAC insert. (B) Schematic of the endogenous Dbx1 locus including intron - exon structure and relative locations of *Bgl*II and *Hind*III restriction sites. (C) The targeting vector used in homologous recombination indicating the positions of the iCre coding sequences, chloramphenicol resistance cassette (Cm^r), loxP sites and the location of the 0.5 kb 3' UTR probe used to hybridize to Southern blots of *Bgl*II – digested genomic DNA. The locations of PCR primers used for genotyping are also indicated. (D) Expression of the iCre transgene at E11.5, revealed by in situ hybridization. Four independent founders had the same pattern of expression at this age. One founder was chosen for further study. (E) Diagram of neuroepithelial precursor domains in the spinal cord, and the reported patterns of Dbx1 and Dbx2 expression at E11.5 (Pierani et al., 2001). FP, floor plate; RP, roof plate.

Figure 2 Defining the limits of GFP expression in *Dbx1-iCre x Rosa26-GFP* offspring. Serial 10 μm sections through the E10.5 upper thoracic spinal cord were subjected to in situ hybridization with various probes or immunohistochemistry for GFP or Pax7. In situ hybridization probes are indicated. (G) shows double-immunolabelling for Pax7 (red) and GFP (green). Brackets (A-C) indicate the approximate limits of the GFP expression domain. Horizontal lines indicate the ventral (D, E F) or dorsal (G, H, I) limits of GFP expression. The ventral limit corresponds approximately to the p2/p1 boundary and the dorsal limit to the dP5/dP4 boundary. Scale bar: 50 μM.

Figure 3 Defining the neuronal subtypes derived from the *Dbx* domain at E12.5. (A) GFP expressing cells (green) migrating laterally (1), ventro-laterally (2) and ventrally (3) from the Dbx expressing region. (B) double immunolabelling for GFP (green) and Isl1/2 (red). (C) GFP and Lim3. (D) GFP and Lbx1. (E) GFP and Evx1. (F) GFP and Lim2. Scale bar: 100 μM

Figure 4 Radial glia are derived from the *Dbx* expressing neuroepithelium. (A, B) GFP expression (green) at E12.5 showing long, fine processes labelled with GFP extending from the ventricular surface to the pial surface (arrows). (C, D) RC2 labelling (red) at E12.5 is seen in many radial glial processes, some of which are also GFP-labelled (E, F, arrows). (G-L) radial glial cell bodies (arrows) appear near the pial surface at E16.5 (G, H, I) and E18.5 (J, K, L). Scale bars: (A) 100 μm (G) 50μm.

Figure 5 Oligodendrocytes are generated from *Dbx*-derived radial glia. Radially orientated GFP-positive cells express the oligodendrocyte lineage markers Olig2 (A, C) and Sox10 (B, D) at E16.5 (A-B) and E18.5 (C-D). Co-localization of the radial glia marker RC2 with GFP-labelled Olig2-positive cells at E15.5 (E, F, G, H) and E16.5 (I, J, K, L) or GFP-labelled Sox10-positive cells at E16.5 (M, N, O, P). Scale bar: 50 μm.

Figure 6 *Dbx*-derived oligodendrocytes at P10. (A) GFP and Sox10 double-immunolabelling. (B) Higher magnification confocal view of the area marked in (A), showing clear co-expression in a subset of Sox10-positive oligodendrocyte lineage cells. (C) GFP and PDGFRa double immuno-labelling. (D) double immuno-labelling of GFP and the differentiated oligodendrocyte marker CC1 (Bhat et al., 1996). Scale bar: 300 μm.

Figure 7 Shh-independent oligodendrocyte development from *Dbx*-derived precursors. Dissociated spinal cords from *Dbx1-iCre x Rosa26-GFP* embryos developed Sox10-positive OLPs within 5 days of culture (A). Their development was not inhibited by cyclopamine (B) but was abolished in the presence of PD173074 (C) or both (D). (E) The experiment was quantified by counting the total number of double-labelled GFP-positive / Sox10-positive cells in the cultures. A minimum of 1000 Sox10-positive cells was counted for each condition. Similar data were obtained in two independent experiments.

Figure 8 Fibrous and protoplasmic astrocytes are derived from the *Dbx* expressing neuroepithelium. (A-B) Co-localization between GFAP (red) and GFP (green) in fibrous astrocytes in the developing white matter of a P10 spinal cord. (B) Confocal microscope view of the area highlighted in (A). (C-F) Protoplasmic astrocytes develop from *Dbx* precursors. (C) All GFP-positive protoplasmic astrocytes co-label with anti-S100β. (D) Protoplasmic astrocytes next to the central canal weakly co-expressed GFAP (arrows). (E-F) GFP (green) and NeuN (red) double labelling in (E) the ventral horn, lying in close proximity to motor neuron cell bodies. (F) Protoplasmic-like astrocytes form bilateral longitudinal columns of cells positioned adjacent to the central canal. Scale bars: (A) 200 μm, (C) 20 μm.

Figure 9 The origins of oligodendrocytes in the embryonic rodent spinal cord. From E12.5 in the mouse, OLPs are generated from pMN in the ventral VZ. Later, from approximately E16, a subsidiary population emerges from radial glial cells in the Dbx1-expressing domain that spans the dorsal-ventral midline. The latter population contributes around 5% of all oligodendrocyte lineage cells in the postnatal cord. Our data do not rule out the possibility that there are additional minor sources of oligodendrocytes outside either pMN or the Dbx domain.

Figure 1 Fogarty et al

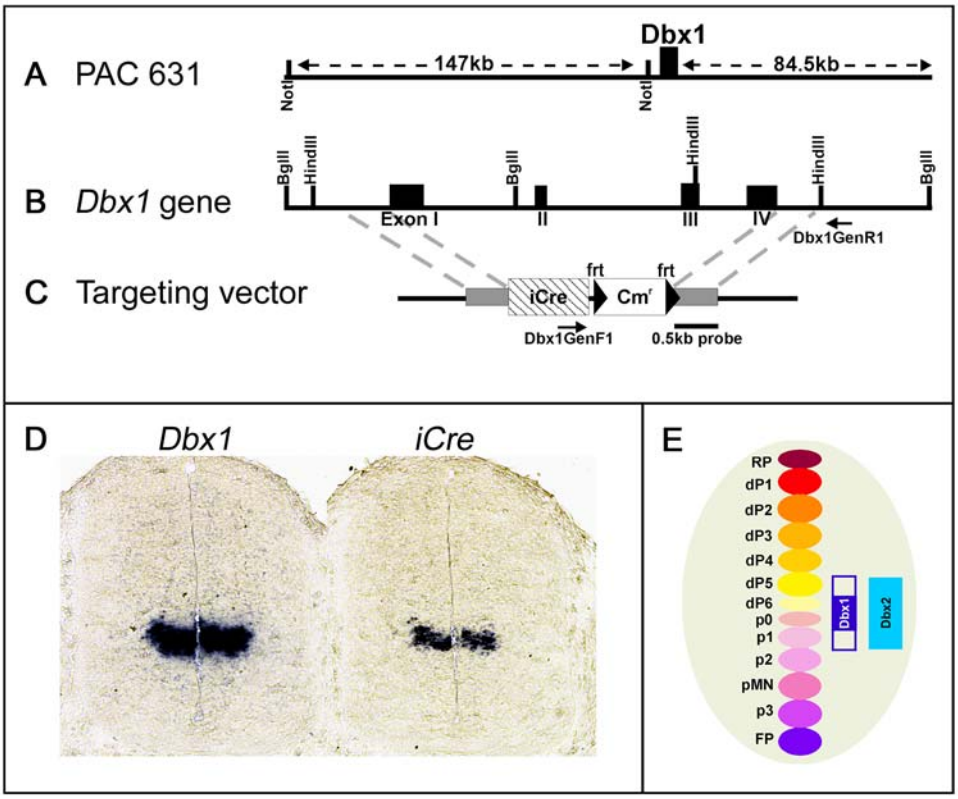

Figure 2 Fogarty et al

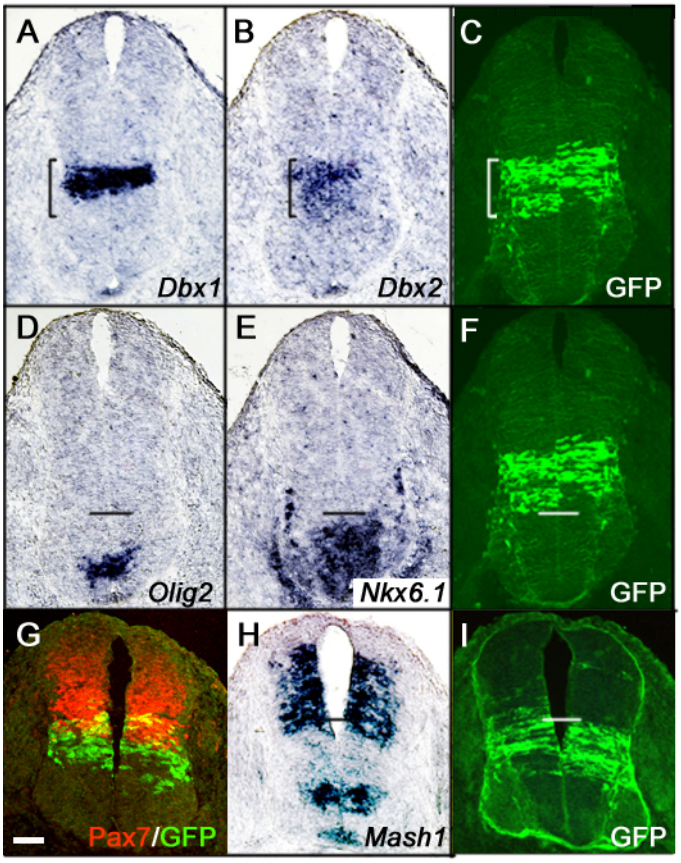

Figure 3 Fogarty et al

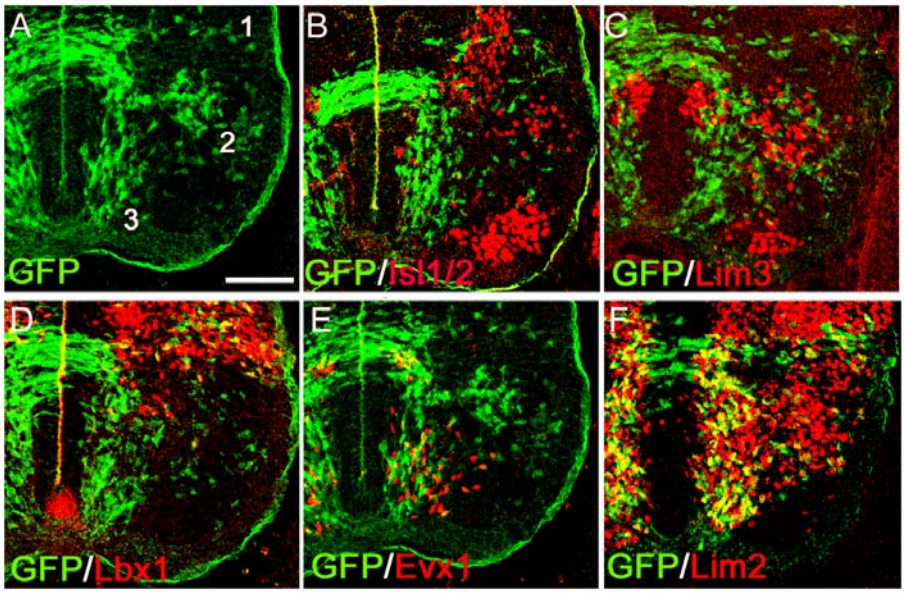

Figure 4 Fogarty et al

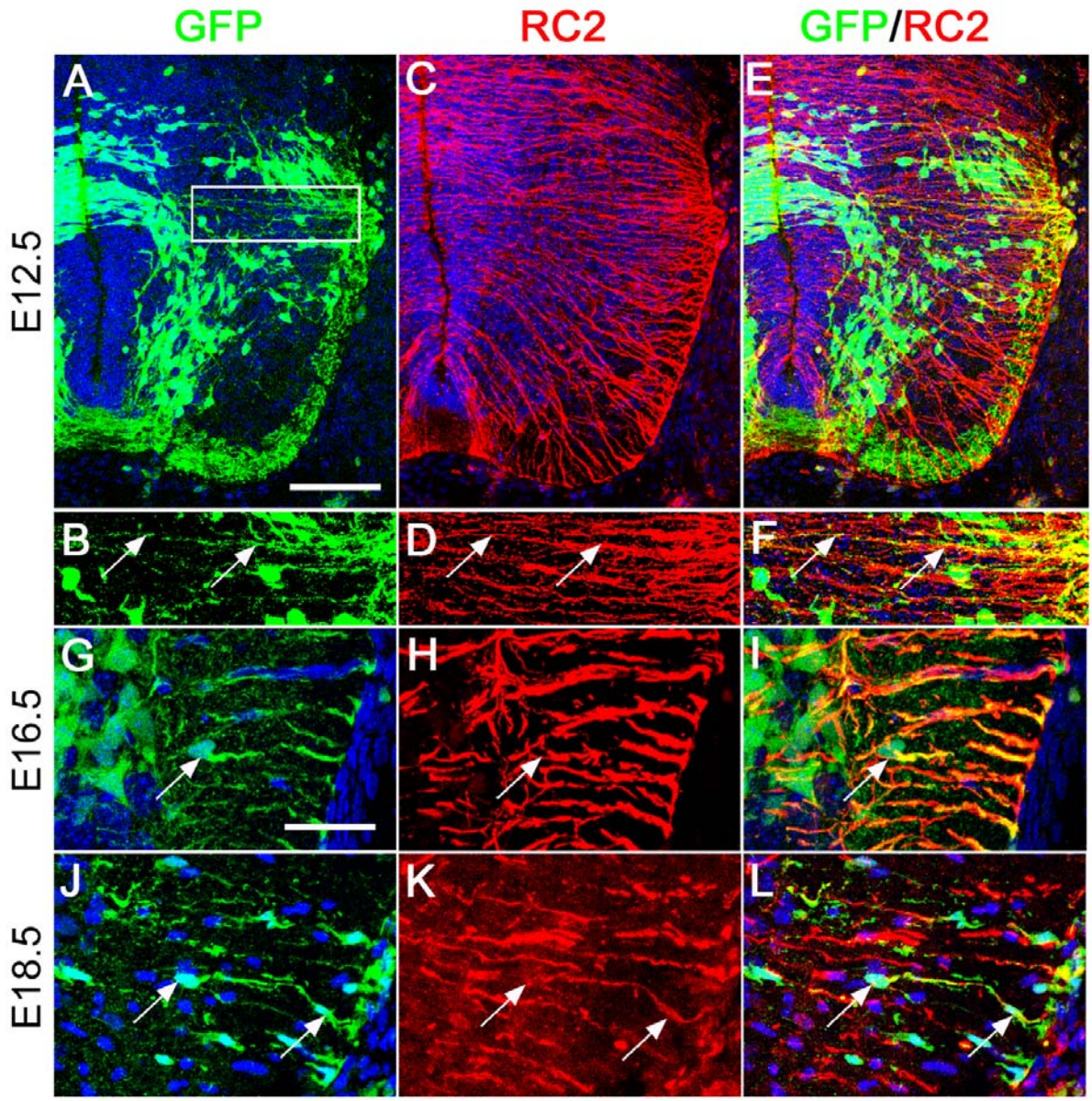

Figure 5 Fogarty et al

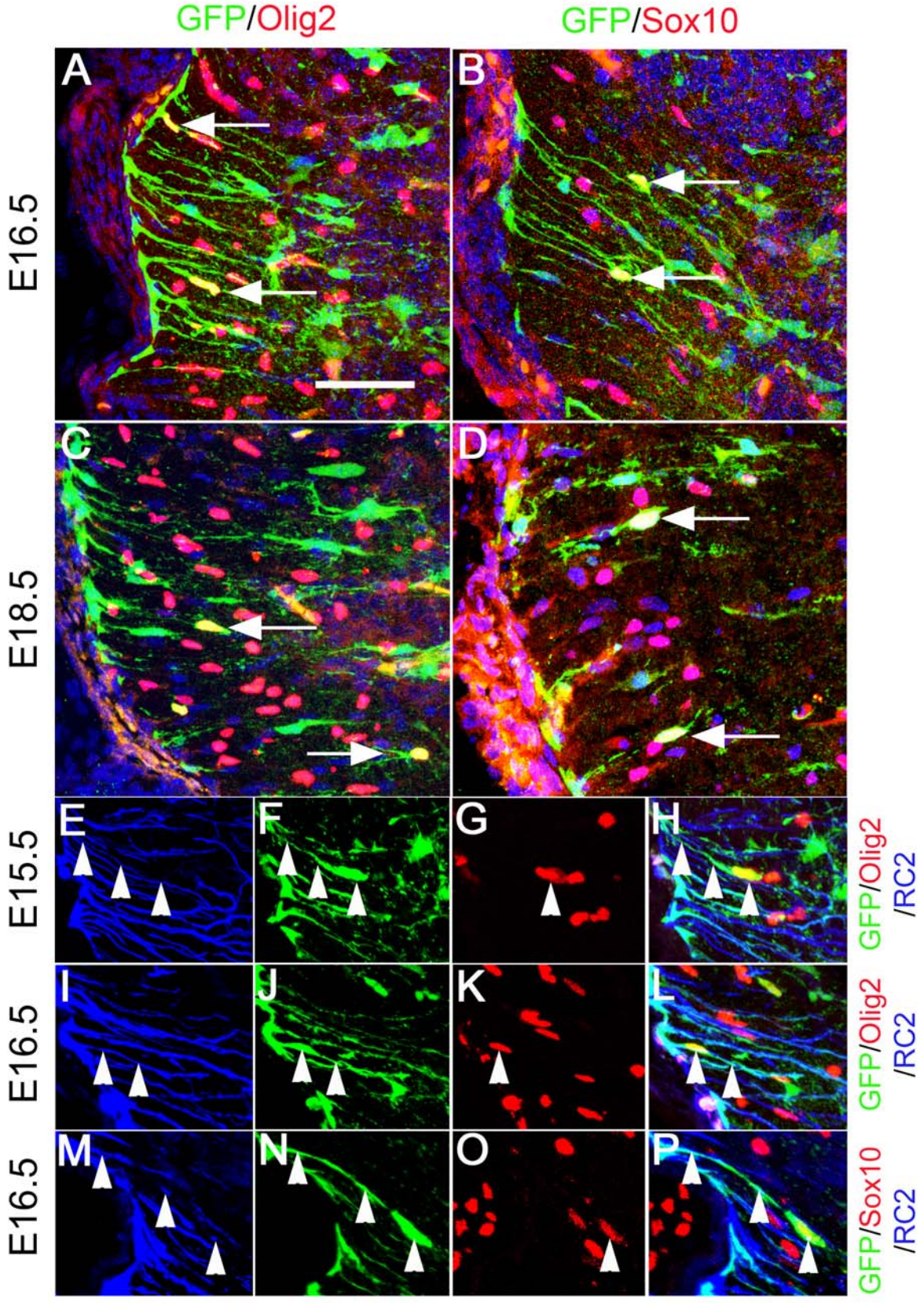

Figure 6 Fogarty et al

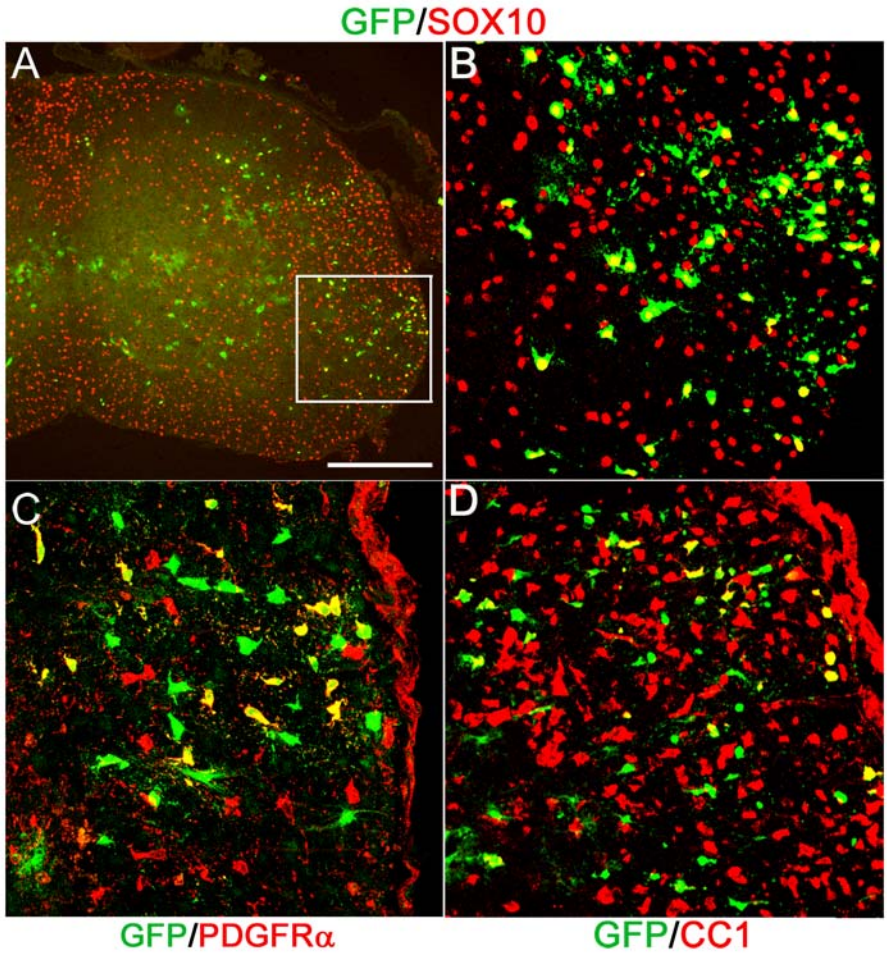

Figure 7 Fogarty et al

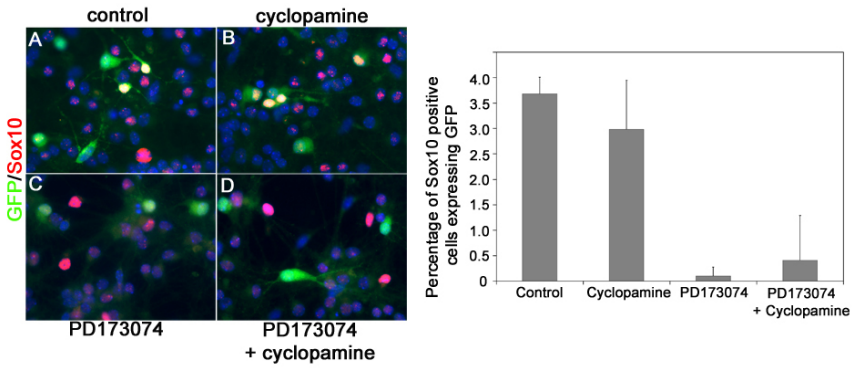

Figure 8 Fogarty et al

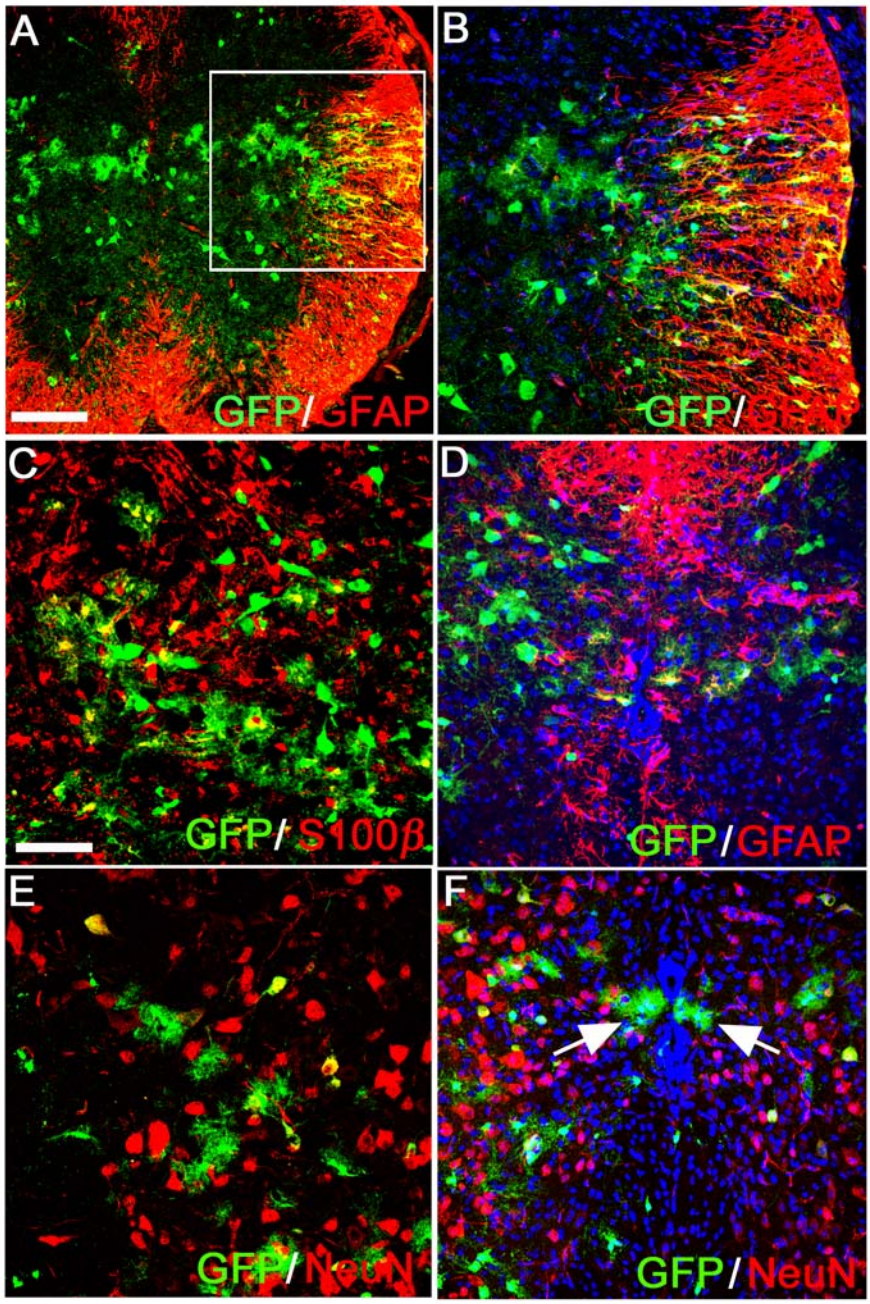

Figure 9 Fogarty et al